Sum rules for resonant inelastic x-ray scattering: Explicit form and angular dependence in perpendicular geometry

F. Borgatti[1,*] G. Ghiringhelli,[2,†] P. Ferriani,[3] G. Ferrari,[3] G. van der Laan,[4] and C. M. Bertoni[3]
[1]*INFM-TASC, Basovizza, S.S. 14, km 163,5, 34012 Trieste, Italy*
[2]*INFM-Dipartmento di Fisica, Politecnico di Milano, p. Leonardo da Vinci 32, 20133 Milano, Italy*
[3]*INFM-Dipartmento di Fisica, Università di Modena e Reggio Emilia, via Campi, Modena, Italy*
[4]*Magnetic Spectroscopy, Daresbury Laboratory, Warrington WA4 4AD, United Kingdom*
(Received 31 July 2003; revised manuscript received 20 January 2004; published 15 April 2004)

Resonant inelastic x-ray scattering (RIXS) and resonant photoemission spectroscopy (RPES) can be used to selectively measure the ground-state properties of atoms in solid materials. For the two types of experiment we compare the sum rules developed in the past years to extract quantitative information from the measured spectra. We show that if the measurements are not sensitive to the emitted photon polarization state (in RIXS) or to the photoelectron spin orientation (in RPES), the two experiments exhibit the same angular dependence of the spectral intensities but differ in some numerical coefficients in the sum rules. In particular we give explicit expressions for the RIXS sum rules in the so-called *perpendicular geometry* for all the cases of practical interest. These rules can serve, in combination with the well-known x-ray magnetic circular dichroism sum rules in absorption, to evaluate the quadrupole and octupole moments of the scattering atoms.

DOI: 10.1103/PhysRevB.69.134420 PACS number(s): 78.70.En, 78.70.Ck, 78.70.Dm

I. INTRODUCTION

Selectivity is among the main virtues of the modern-day resonant spectroscopies that are emerging from the development of synchrotron-radiation instrumentation. The tunability of the photon energy allows selection of the chemical element and the character of the valence states participating in the excitation process. Also the high degree of polarization of synchrotron radiation can be exploited in a wide variety of applications. For example, left and right circularly polarized photons are absorbed with different probability in an atom that has a magnetic moment along the photon propagation direction. This phenomenon, known as x-ray magnetic circular dichroism (XMCD) in absorption,[1,2] has been exploited, together with x-ray magnetic linear dichroism,[3] to study the magnetic properties of bulk solids and thin films.

Further selectivity can be added by choosing the decay channel following the x-ray absorption: resonant photoemission spectroscopy (RPES) and resonant inelastic x-ray scattering (RIXS) are processes in which a nonradiative (Auger like) and a radiative decay channel is involved, respectively. In this case, the propagation direction, energy, and polarization state of the emitted particles (photons or electrons, respectively) increase the selectivity of the process. These scattering processes can be adequately described using a second-order formalism, where the two steps (excitation and decay) interfere with each other via the set of intermediate states. For both RPES and RIXS the Kramers-Heisenberg[4–6] formula has been used extensively and with great success.[7–12]

In recent years, the interest in the resonant excitation processes has stimulated theoretical efforts to develop sum rules for RPES and RIXS, similar to those used widely in XMCD.[13–15] Such rules are precious tools to extract *quantitative* information from the experimental spectra without the need of numerical calculations. The higher-order process of the scattering compared to absorption and the additional selectivity of the scattering channel allow us to access a wider range of quantities related to the charge and magnetic properties of the partially filled shells in the ground state (the physical meaning of the most common ones is summarized in Table I).

The theoretical analysis of RPES and its sum rules by van der Laan and Thole[16] was followed by experimental work[17,18] and by detailed model calculations.[19] An interesting new type of magnetic circular dichroism (MCD) was observed in Ni,[17] Fe,[20] and Tb (Ref. 21) metal with the sample magnetization oriented perpendicular to the incident photons. We will refer to this type of setup as the *perpendicular geometry*. Although the XMCD in absorption vanishes in this geometry, a significant dichroic signal can be present in the decay channel. For RIXS a theoretical description was presented by Carra *et al.*[22] and van Veenendaal *et al.*[23] RIXS-MCD in perpendicular geometry at the Ni and Co L_3 edges was first observed by Braicovich *et al.*[24] and confirmed for Gd L_3 by Fukui *et al.*[25] The first quantitative use of the RIXS-MCD sum rules was done only very recently and was made possible by using a dedicated experimental apparatus.[26,27] On the other hand, in Ref. 27 the use of the RPES sum rules has been extended to RIXS.

In this work we compare RIXS and RPES cross sections and we provide detailed formulas and tables for the application of the RIXS sum rules in the so-called perpendicular geometry using circularly polarized light. We are motivated by the strong similarity of the scattering operators present in RIXS and RPES expressions [see, e.g., Eq. (30) in Ref. 23 and Eq. (10) in Ref. 28] as of the terms concerning the angular dependence of the incident/emitted particles. Despite the different kind of the deexcitation process it may be argued that when the measurements are not sensitive to the internal degrees of freedom of the emitted particles, i.e., the photon polarization (as in usual RIXS experiments) or the electron spin, but only to their propagation direction, the two processes become somehow equivalent therefore resulting in the same sum rules. We show that this is not strictly exact. Slightly different quantitative results are obtained when using RPES sum rules instead of the RIXS ones. The differ-

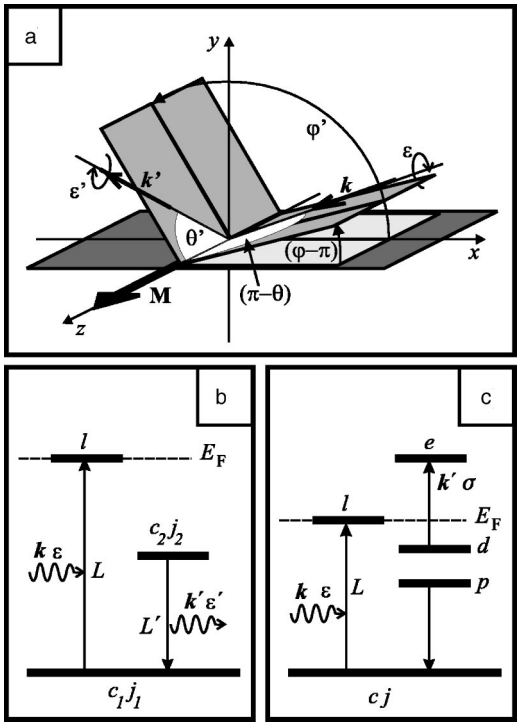

FIG. 1. (a) Schematic representation of the scattering geometry for a generic case. The incident and the scattered photons are polarized and their wave vectors **k** and **k**′ are given by (θ,φ) and (θ',φ'). The quantization axis and sample magnetization is along **z**. (b) The diagram of the excitation and decay steps in a single-particle representation for RIXS. (c) Same for RPES. See text for more details.

ences between RIXS and RPES sum rules arise from to the presence of some numerical coefficients involving high-order multipole moments. Thus the recent results obtained from RIXS measurements[27] might require only minor corrections (comparable with the experimental errors) that will not significantly affect the approach followed in those works, although this is not generally true. To this aim we write the RIXS cross section (integrated over the energy of the photons emitted in a selected decay channel) and the associated sum rules in a general form which is also suitable for the experimentalists to select the most useful scattering process and geometry for the case of interest. To complete our work, we calculate the explicit expressions for all possible excitation and decay channels that are reasonably accessible in magnetic systems in perpendicular geometry, which is a particularly convenient way to measure RIXS-MCD. In fact, in any different arrangement the absorption XMCD would largely dominate the signal, making the task of measuring higher-order multipole moments even harder. In this way we provide a complete framework for the application of the RIXS sum rules in perpendicular geometry to all cases of interest.

The paper is structured as follows. In Sec. II we compare the RIXS and RPES integrated cross sections and all the quantities involved in these processes. In Sec. III we apply the RIXS sum rules to the case of perpendicular geometry. We show the quantities to be corrected with respect to the results obtained by RPES theory. The conclusions follow in Sec. IV. In the appendixes we provide complete reference tables for all the scattering processes of interest.

II. RIXS VS RPES

We will not enter into any theoretical discussion on the models but start from the results of Refs. 16, 17, 22, and 23. We just mention that both theories have been developed in the fast-collision approximation, i.e., under the assumption that second-order resonant processes are so fast that the excitation and decay steps are practically simultaneous. For a discussion of this approximation we refer to Refs. 6, 16, 29, and 30 and references therein.

The schemes for the (one-electron) resonant processes are illustrated in Fig. 1. The scattering geometry in the laboratory reference system is displayed in 1(a). The target atom is located at the origin. Its quantization axis **z** coincides with the magnetization vector, to which the atomic magnetic moment is aligned. The incident photon has polarization $\boldsymbol{\epsilon}$, wave vector **k**, and energy $\hbar\omega_{\mathbf{k}}$. The scattering process intrinsic to the target atom is shown in 1(b). The electric 2^L-pole transition of the resonant excitation process promotes a core electron with orbital and angular quantum numbers $(c_1, j_1 = c_1 \pm \frac{1}{2})$ to an open (valence) shell with orbital quantum number l, where $|l - c_1| = L$. The core hole (c_1, j_1) is filled by an electron decaying from the core shell (c_2, j_2) through an electric $2^{L'}$-pole transition, where $|c_1 - c_2| = L'$. The emitted photon has polarization $\boldsymbol{\epsilon}'$, wave vector $\mathbf{k}'$, and energy $\hbar\omega_{\mathbf{k}'}$. In the scattering event the energy transfer to

TABLE I. Physical meaning of the operators $\underline{w}^{abr}$. The listed quantities refer to the *hole* properties (Refs. 23 and 30). The physical meaning of these operators for the *electron* representation may be found in Ref. 34.

$\underline{w}^{abr}$	p shell	d shell	f shell	Meaning
$\underline{w}^{000}$	n_h	n_h	n_h	Number of holes
$\underline{w}^{110}$	$-2l\cdot s$	$-l\cdot s$	$-\frac{2}{3}l\cdot s$	Isotropic spin-orbit coupling
$\underline{w}^{011}$	$2S_z$	$2S_z$	$2S_z$	Spin moment
$\underline{w}^{101}$	L_z	$\frac{1}{2}L_z$	$\frac{1}{3}L_z$	Orbital moment
$\underline{w}^{211}$	$5T_z$	$\frac{7}{2}T_z$	$3T_z$	Magnetic-dipole term
$\underline{w}^{112}$	$3P_{zz}$	$\frac{3}{2}P_{zz}$	P_{zz}	Anisotropic spin-orbit coupling
$\underline{w}^{202}$	$3Q_{zz}$	$\frac{1}{2}Q_{zz}$	$\frac{1}{5}Q_{zz}$	Charge quadrupole
$\underline{w}^{312}$		R_{zz}	$\frac{3}{10}R_{zz}$	Higher-order quadrupole

the system is $(\hbar\omega_{\mathbf{k}}-\hbar\omega_{\mathbf{k}'})$. For RPES the mechanism is shown in (c) of Fig. 1. The excitation step for the electric 2^L-pole radiative transition is the same. The core and valence shell are labeled by quantum numbers in the same way as in RIXS. After excitation the atom emits an electron through a nonradiative Auger process leaving the system in a two-hole final state. The emitted electron is characterized by the propagation direction $\hat{\mathbf{k}}'$ and direction $\mathbf{P}_S$ along which the spin polarization is measured.

We are interested to compare the RIXS and RPES cross sections *integrated over the energy* $\hbar\omega_{\mathbf{k}'}$ *of the emitted particles for the specific decay channel* and for a magnetic system with negligible crystal-field interaction (i.e., SO_2 symmetry[31,32]). To do that we put the RIXS formula in a general form comparable to the RPES, the latter being written in the same notation used for the RIXS theory.[33] In particular for RIXS we write the terms related to the angular dependence in a more appropriate form than in Ref. 23. Because most of the experiments performed up to now in magnetic systems use circularly polarized incident radiation we consider only the case of pure circular polarization. We obtain

$$J_{\mu}^{\mathrm{RIXS}}=\mathbb{N}(l,L,L',\omega)\sum_{\mu' zz' r}(-1)^{z+z'}\left[\frac{z,z'}{r}\right]^{1/2}\times C^{z0}_{L\mu,L-\mu}C^{z'0}_{L'\mu',L'-\mu'}\mathbb{E}^{zz'r}_{j_1}(c_1,l,L)\times\tilde{\mathcal{B}}^{z'}_{j_1,j_2}(c_1,c_2,L')\Theta^{zz'r}(\hat{\mathbf{k}},\hat{\mathbf{k}}'),\tag{1}$$

$$J_{\mu}^{\mathrm{RPES}}=\frac{1}{4\pi}\sum_{zz'r}(-1)^{z+z'}\left[\frac{z,z'}{r}\right]^{1/2}C^{z0}_{L\mu,L-\mu}\mathbb{E}^{zz'r}_{j_1}(c_1,l,L)\times\mathcal{B}^{z'0z'}_{j}(LS)\Theta^{zz'r}(\hat{\mathbf{k}},\hat{\mathbf{k}}'),\tag{2}$$

where $\mu(\mu')=\pm1$ denotes the right $(+1)$ and left (-1) circular polarization state of the incident (scattered) photon and where we used the short-hand notation $[a,\ldots,b]=(2a+1)\cdots(2b+1)$.

The explicit form of the symbols and the integer range of all the indices are listed in Appendix A. In both formulas all terms have been grouped corresponding to their physical meaning. The $\mathbb{N}(l,L,L',\omega)$ prefactor is a global normalization term including the dependence on the incident photon energy. The factor $\mathbb{E}^{zz'r}$ is related to the transition probability of the excitation step. It consists of linear combinations of $\underline{w}^{abr}_0$ tensors[34,35] which provide the physical information on the *ground-state* valence electron distribution. The relation between the LS-coupled tensor operators $\underline{w}^{abr}$ in the *hole* representation and the standard ground-state operators is shown in Table I. The $\tilde{\mathcal{B}}^{z'}_{j_1,j_2}$ and $\mathcal{B}^{z'0z'}_{j}$ factors are related to the transition probabilities of the decay channels. Obviously, they are defined differently (see Ref. 23 and Ref. 16, respectively) but the physical meaning is definitively the same. The geometrical dependence on the incident and emitted particle directions with respect to the magnetization direction is given by $\Theta^{zz'r}(\hat{\mathbf{k}},\hat{\mathbf{k}}')$. In the absence of spin- or light-polarization detection only terms with z' even contribute to both cross sections.

Apart from the global prefactors and the decay strengths, the main differences in Eqs. (1) and (2) arise from factors related to the nature of the emitted particle and the way in which the integration over the photon polarization state or the electron-spin direction is performed. The photon has two polarization states defined with respect to its propagation direction, so that in Eq. (1) a sum over both states $(\mu'=\pm1)$ is required. In Eq. (2) the factor $C^{z'0}_{L'\mu',L'-\mu'}$ and the associated sum over μ' are absent because the emitted particle is an electron, whereas the factor $C^{z0}_{L\mu,L-\mu}$ for the incident photon is still present. To account for all possible spin directions in Eq. (2) an angular integration over the solid angle must be performed,[16] resulting in the disappearing of any angular spin dependence from Eq. (2). Consequently, J^{RIXS} and J^{RPES} cross sections are not completely equivalent implying the small differences between the respective sum rules (an example is given in the following section).

III. RIXS-MCD SUM RULES IN PERPENDICULAR GEOMETRY

We present the expressions that can be applied to the RIXS experimental data by taking the sum and difference over the incident polarization states: $J^{\mathrm{RIXS}}_{\mathrm{sum}}=(J_{+1}+J_{-1})$ and $J^{\mathrm{RIXS}}_{\mathrm{dif}}=(J_{+1}-J_{-1})$. Using Eq. (1) we computed $J^{\mathrm{RIXS}}_{\mathrm{sum}}$ and $J^{\mathrm{RIXS}}_{\mathrm{dif}}$ for a number of allowed resonant excitations and successive decay channels. We assume that the sample is magnetized along the **z** axis and that the incident photons propagate along the $-\mathbf{x}$ direction (c.f. Fig. 1). Since the photons are circularly polarized this corresponds to the *perpendicular geometry*, where the XMCD in absorption vanishes and the dichroism is entirely due to interference in the second-order process. We write $J^{\mathrm{RIXS}}_{\mathrm{sum}}$ and $J^{\mathrm{RIXS}}_{\mathrm{dif}}$ as a function of the emitted photon propagation direction, given by the spherical coordinates θ' and φ' as defined in Fig. 2 $(0\leqslant\theta'<\pi;\ 0\leqslant\varphi'<2\pi)$. We have considered all the allowed resonant excitations with an *s*, *p*, or *d* core hole in the intermediate state, as obtained from the electric dipole $(E1)$ and quadrupole $(E2)$ radiative excitations, and all the possible $E1$ radiative decays.[36] Comparison of all the results allow us to make some important comments concerning the general properties of $J^{\mathrm{RIXS}}_{\mathrm{sum}}$ and $J^{\mathrm{RIXS}}_{\mathrm{dif}}$ and about the optimal experimental conditions for the sum-rule application.

First of all, in perpendicular geometry we can rewrite the sum and difference signal in the simple form

$$J^{\mathrm{RIXS}}_{\mathrm{sum}}=\frac{k}{6}[C_0+C_1(3\cos^2\theta'-1)+C_2\cos2\varphi'\sin^2\theta'],\tag{3}$$

$$J^{\mathrm{RIXS}}_{\mathrm{dif}}=-k\,C_3\cos\varphi'\sin2\theta',\tag{4}$$

where the coefficients k and C_i depend on the selected excitation and decay transitions.

The coefficient C_i can be written as $C_i\propto A_i\mathcal{B}^j$, where the A_i term depends on the excitation process and the $\mathcal{B}^j$ on the decay channel. The explicit expressions for C_i are given in Appendix B. They are ultimately given by a linear combination of multipole moments $\underline{w}^{abr}$. Here we mention that if

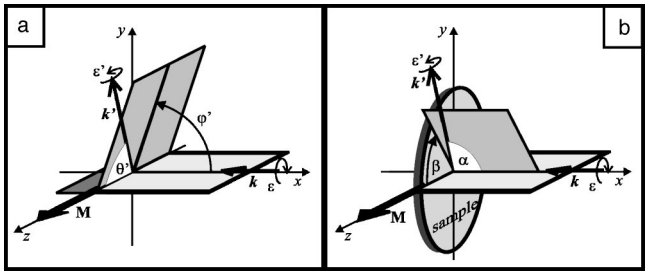

FIG. 2. (a) Schematic representation of the scattering geometry in perpendicular geometry. The incident circularly polarized photon propagates along $-\mathbf{x}$. The scattered photon wave vector $\mathbf{k}'$ is described by (θ',φ'). The quantization axis and sample magnetization are along $\mathbf{z}$. (b) The perpendicular geometry in the case of a conical scan. The scattered photon is emitted along $\mathbf{k}$ with angles (α,β). The conical scan is particularly convenient when the sample normal is along $\mathbf{x}$.

$j_1<1$ (i.e., $j_1=\frac{1}{2}$ at the K, L_1, L_2, M_1, and M_2 absorption edges) only the coefficient C_0 is nonzero because $\mathcal{B}^2=0$ for an $s_{1/2}$ and $p_{1/2}$ hole in the intermediate state. In those cases there is no dichroism nor any modulation of the $J_{\rm sum}^{\rm RIXS}$ signal in perpendicular geometry.

The numerical factor k may be written as $k=8\pi\lambda^2|\mathcal{A}(\omega_{\mathbf{k}})|^2K_1K_2/(256\pi^2)$, where K_1 depends on the excitation and K_2 on the decay (see Table V). The absolute amplitude of the RIXS signal depends on the principal quantum number n of the levels involved in the process, and this dependence is implicitly expressed by the reduced scattering amplitude $\mathcal{A}(\omega_{\mathbf{k}})$ via the incident photon energy $\omega_{\mathbf{k}}$. This means that the choice of the specific absorption edge is not only determined by the convenience of the RIXS sum-rule analysis, but also by the absolute cross section, e.g., for $3d$ transition metals the RIXS signal is at least two orders of magnitude lower at the $M_{2,3}$ edges than at the $L_{2,3}$ edges.

We can now compare the theories of RIXS and RPES. If we apply the results of Sec. II to the L_3 absorption edge of a $3d$ transition metal,[37] it emerges that Eqs. (3) and (4) are also valid for RPES, but that the C_0 factor is different: $C_0^{\rm RPES}=4A_0^{E1}\mathcal{B}^0$, i.e., $\frac{1}{2}$ (the listed value from Table II), whereas all the other C_i factors are identical. This example demonstrates that if the RPES sum rules would be applied to RIXS measurements, all the quantities included in the C_0 factor are estimated wrongly. Clearly, the expression of the factor $\mathcal{B}^0$ is different for RPES and for RIXS, as well as the value of k.

Looking at Eqs. (3) and (4) we see that the modulations of $J_{\rm sum}$ and $J_{\rm dif}$ have the form of spherical harmonics. In particular, $J_{\rm sum}$ is modulated by $Y_{2,0}$ and Re$[Y_{2,2}]$, while $J_{\rm dif}$ is modulated by Re$[Y_{2,1}]$, corresponding to d_{z^2}, $d_{x^2-y^2}$, and d_{zx} orbitals, respectively. Thus the $J_{\rm sum}^{\rm RIXS}$ signal is even with respect to the xy, yz, and zx planes, while $J_{\rm dif}^{\rm RIXS}$ is odd with respect to the xy and yz planes, and even with respect to the zx plane. $J_{\rm dif}^{\rm RIXS}$ is zero along the three axes and maximum along the bisector of the $\widehat{xz}$ angle: the maximum of the RIXS dichroism can be detected along the 45° back-scattering direction in the zx plane. It must be noted that the angular dependence given in Eqs. (3) and (4) is only valid under the fast-collision approximation. Outside that assumption the general expressions of the scattering cross section display a more complicated dependence on the angles (θ',ϕ'), e.g., $J_{\rm dif}$ is no longer symmetric with respect to the zx plane so that the reversal of the magnetization and the reversal of the incident photon polarization are no longer equivalent operations.[30] The symmetry of $J_{\rm dif}$ with respect to the zx plane could therefore be used as a test for the validity of the fast-collision approximation case by case.

When the scattering is restricted to the zx plane $(\varphi'=0)$, i.e., in-plane with the sample magnetization and incident photon beam, Eqs. (3) and (4) obtain a very simple form. For this so called *in-plane perpendicular geometry* the angular dependence of $J_{\rm dif}^{\rm RIXS}$ was studied theoretically and experimentally at the Gd L_3 edge by Fukui *et al.*[25,38] and at the Co L_3 edge by Tagliaferri *et al.*[39]

Finally, we recall that RIXS measurements, especially in the soft x-ray region, are strongly influenced by self-absorption, i.e., by reabsorption of the scattered photons by the sample. Self-absorption varies considerably with the angle between the scattering direction and the sample surface. In those experiments where the scattering direction is scanned to measure the modulation of $J_{\rm sum}^{\rm RIXS}$ Braicovich *et al.*[27] found it very convenient to keep a fixed angle between scattered photons and the sample surface. The artefacts due to self-absorption are minimized and kept constant by scanning the scattering direction on a cone with its axis along the $\hat{\mathbf{x}}$ direction (*conical scan*). The expressions for the sum and difference signal can be written as

$$J_{\rm sum}^{\rm RIXS}=\frac{k}{6}\left[C_0+\frac{C_1-C_2}{2}(3\sin^2\alpha-2)+\frac{3C_1+C_2}{2}\sin^2\alpha\cos 2\beta\right], \quad (5)$$

TABLE II. Explicit form of the coefficients C_i in Eqs. (3)–(6) for electric dipole and quadrupole transitions.

	$E1$	$E2$
C_0	$8A_0^{E1}\mathcal{B}^0$	$8(A_0^{E1}+A_0^{E2})\mathcal{B}^0$
C_1	$2A_1^{E1}\mathcal{B}^2$	$2(A_1^{E1}+A_1^{E2})\mathcal{B}^2$
C_2	$A_2^{E1}\mathcal{B}^2$	$(A_2^{E1}+A_2^{E2})\mathcal{B}^2$
C_3	$A_3^{E1}\mathcal{B}^2$	$(\frac{2}{3}A_3^{E1}+A_3^{E2})\mathcal{B}^2$

TABLE III. Definition of the factors A_i^{EL} (in Table II) for electric dipole and quadrupole transitions. They contain the physical information about the atomic properties given by linear combinations of $\underline{w}^{abr}$ (see Table IV).

A_0^{E1}	$4\mathbb{E}^{000}-\mathbb{E}^{202}$
A_1^{E1}	$4\mathbb{E}^{022}-(\mathbb{E}^{220}+\mathbb{E}^{222}+\mathbb{E}^{224})$
A_2^{E1}	$6\mathbb{E}^{220}-6\mathbb{E}^{222}+\mathbb{E}^{224}$
A_3^{E1}	$3\mathbb{E}^{121}-2\mathbb{E}^{123}$
A_0^{E2}	$\frac{1}{7}(17\mathbb{E}^{202}-3\mathbb{E}^{404})$
A_1^{E2}	$\frac{17}{7}(\mathbb{E}^{220}+\mathbb{E}^{222}+\mathbb{E}^{224})-\frac{3}{7}(\mathbb{E}^{422}+\mathbb{E}^{424}+\mathbb{E}^{426})$
A_2^{E2}	$-\frac{17}{7}(6\mathbb{E}^{220}-6\mathbb{E}^{222}+\mathbb{E}^{224})+\frac{2}{7}(5\mathbb{E}^{422}-9\mathbb{E}^{424}+2\mathbb{E}^{426})$
A_3^{E2}	$\frac{1}{6}(8\mathbb{E}^{321}+3\mathbb{E}^{323}-6\mathbb{E}^{325})$

TABLE IV. Explicit expressions for $\mathbb{E}^{zz'r}$ [Eq. (A2)] as linear combination of the ground-state moments $\underline{w}^{abr}$. Listed are the $zz'r$ combinations needed in perpendicular geometry for the absorption edges (first column) corresponding to a core hole with arbitrary principal quantum number n but same (c_1, j_1) (second column) in the intermediate state.

Edges	Hole	c_1	j_1	$zz'r$	$\mathbb{E}^{zz'r}$
K,L_1,M_1,N_1	$s_{1/2}$	0	$\frac{1}{2}$	000	$\underline{w}^{000}$
				202	$\underline{w}^{202}$
				404	$\underline{w}^{404}$
L_2,M_2,N_2	$p_{1/2}$	1	$\frac{1}{2}$	000	$\underline{w}^{000}-\underline{w}^{110}$
				202	$-\frac{1}{5}(2\underline{w}^{112}-5\underline{w}^{202}+3\underline{w}^{312})$
				404	$-\frac{1}{9}(4\underline{w}^{314}-9\underline{w}^{404}+5\underline{w}^{514})$
L_3,M_3,N_3	$p_{3/2}$	1	$\frac{3}{2}$	000	$2\underline{w}^{000}+\underline{w}^{110}$
				220	$\frac{1}{5}(\underline{w}^{000}+2\underline{w}^{110})$
				121	$\frac{2}{15}(5\underline{w}^{011}+3\underline{w}^{101}+\underline{w}^{211})$
				321	$\frac{9}{35}(\underline{w}^{101}+2\underline{w}^{211})$
				022	$2\underline{w}^{112}+\underline{w}^{202}$
				202	$\frac{1}{5}(2\underline{w}^{112}+10\underline{w}^{202}+3\underline{w}^{312})$
				222	$\frac{2}{35}(7\underline{w}^{112}+5\underline{w}^{202}+3\underline{w}^{312})$
				422	$\frac{2}{7}(\underline{w}^{202}+2\underline{w}^{312})$
				123	$\frac{3}{5}(2\underline{w}^{213}+\underline{w}^{303})$
				323	$\frac{4}{105}(9\underline{w}^{213}+7\underline{w}^{303}+5\underline{w}^{413})$
				224	$\frac{18}{35}(2\underline{w}^{314}+\underline{w}^{404})$
				404	$\frac{1}{9}(4\underline{w}^{314}+18\underline{w}^{404}+5\underline{w}^{514})$
				424	$\frac{20}{693}(11\underline{w}^{314}+9\underline{w}^{404}+7\underline{w}^{514})$
				325	$\frac{10}{21}(2\underline{w}^{415}+\underline{w}^{505})$
				426	$\frac{5}{11}(2\underline{w}^{516}+\underline{w}^{606})$
M_4,N_4	$d_{3/2}$	2	$\frac{3}{2}$	000	$2(\underline{w}^{000}-\underline{w}^{110})$
				220	$\frac{2}{5}(\underline{w}^{000}-2\underline{w}^{110})$
				121	$-\frac{4}{15}(\underline{w}^{011}-3\underline{w}^{101}+2\underline{w}^{211})$
				022	$-\frac{2}{5}(2\underline{w}^{112}-5\underline{w}^{202}+3\underline{w}^{312})$
				202	$-\frac{2}{5}(\underline{w}^{112}-5\underline{w}^{202}+3\underline{w}^{312})$
				222	$-\frac{4}{35}(2\underline{w}^{112}-5\underline{w}^{202}+3\underline{w}^{312})$
				123	$-\frac{6}{35}(3\underline{w}^{213}-7\underline{w}^{303}+4\underline{w}^{413})$
				224	$-\frac{4}{35}(4\underline{w}^{314}-9\underline{w}^{404}+5\underline{w}^{514})$
M_5,N_5	$d_{5/2}$	2	$\frac{5}{2}$	000	$3\underline{w}^{000}+2\underline{w}^{110}$
				220	$\frac{1}{25}(12\underline{w}^{000}+13\underline{w}^{110})$
				121	$\frac{2}{75}(28\underline{w}^{011}+36\underline{w}^{101}+11\underline{w}^{211})$
				022	$\frac{1}{25}(56\underline{w}^{112}+60\underline{w}^{202}+9\underline{w}^{312})$
				202	$\frac{1}{5}(4\underline{w}^{112}+15\underline{w}^{202}+6\underline{w}^{312})$
				222	$\frac{2}{175}(41\underline{w}^{112}+60\underline{w}^{202}+24\underline{w}^{312})$
				123	$\frac{3}{175}(79\underline{w}^{213}+84\underline{w}^{303}+12\underline{w}^{413})$
				224	$\frac{6}{175}(34\underline{w}^{314}+36\underline{w}^{404}+5\underline{w}^{514})$

$$J_{\mathrm{dif}}^{\mathrm{RIXS}} = -kC_3 \sin 2\alpha \cos\beta, \tag{6}$$

with the angles α and β as defined in (b) of Fig. 2 ($0 \leqslant \alpha < \pi$; $0 \leqslant \beta < 2\pi$) In a conical scan, α is fixed and only the dependence on β is measured. This type of scan has not only advantages for practical reasons (self-absorption artefacts are eliminated) but also for the application of the RIXS sum rules. In fact, the term $(3C_1+C_2)$ is given by a linear combination of $\underline{w}^{abr}$ tensors with only r is 2 and 4, so that the magnitude of the modulation for J_{sum} provides a direct measurement of the quadrupole tensors (neglecting higher-order tensors that are usually much smaller). The choice of α can be decided by practical considerations. For example, for $\alpha = \pi/4$ the dichroism $J_{\mathrm{dif}}^{\mathrm{RIXS}}$ is maximized, while at the *magic* angle ($\sin^2\alpha = \frac{2}{3}$) the term $\frac{1}{2}(C_1 - C_2)$ in $J_{\mathrm{sum}}^{\mathrm{RIXS}}$ disappears.

IV. CONCLUSIONS

The interest in the second-order resonant processes has stimulated the development of sum rules for quantitative

TABLE V. The values of the numerical coefficients K_1, K_2, $\mathcal{B}^0$, and $\mathcal{B}^2$ (in Table II) for all the considered excitation (first column) and decay (fourth column) combinations.

Hole	K_1^{E1}	K_1^{E2}	Decay	K_2	$\mathcal{B}^0$	$\mathcal{B}^2$	$\mathcal{B}^2/\mathcal{B}^0$
$s_{1/2}$	1	$\sqrt{\frac{3}{5}}$	$p_{1/2}\rightarrow s_{1/2}$	1	1	0	0
			$p_{3/2}\rightarrow s_{1/2}$	1	2	0	0
			$p\rightarrow s_{1/2}$	1	3	0	0
$p_{1/2}$	$\frac{1}{\sqrt{5}}$	$\frac{1}{\sqrt{7}}$	$s_{1/2}\rightarrow p_{1/2}$	1	1	0	0
			$d_{3/2}\rightarrow p_{1/2}$	$\frac{1}{\sqrt{5}}$	5	0	0
$p_{3/2}$	$\frac{1}{\sqrt{5}}$	$\frac{1}{\sqrt{7}}$	$s_{1/2}\rightarrow p_{3/2}$	1	1	1	1
			$d_{3/2}\rightarrow p_{3/2}$	$\frac{1}{\sqrt{5}}$	$\frac{1}{2}$	$-\frac{2}{5}$	$-\frac{4}{5}$
			$d_{5/2}\rightarrow p_{3/2}$	$\frac{1}{\sqrt{5}}$	$\frac{9}{2}$	$\frac{9}{10}$	$\frac{1}{5}$
			$d\rightarrow p_{3/2}$	$\frac{1}{\sqrt{5}}$	5	$\frac{1}{2}$	$\frac{1}{10}$
$d_{3/2}$	$\frac{3}{5\sqrt{21}}$		$p_{1/2}\rightarrow d_{3/2}$	1	$\frac{5}{2}$	$\frac{5}{2}$	1
			$p_{3/2}\rightarrow d_{3/2}$	1	$\frac{1}{2}$	$-\frac{2}{5}$	$-\frac{4}{5}$
			$p\rightarrow d_{3/2}$	1	3	$-\frac{21}{10}$	$-\frac{7}{10}$
			$f_{5/2}\rightarrow d_{3/2}$	$\sqrt{\frac{3}{7}}$	7	$\frac{7}{5}$	$\frac{1}{5}$
$d_{5/2}$	$\frac{3}{5\sqrt{21}}$		$p_{3/2}\rightarrow d_{5/2}$	1	3	3	1
			$f_{5/2}\rightarrow d_{5/2}$	$\sqrt{\frac{3}{7}}$	$\frac{1}{3}$	$-\frac{8}{21}$	$-\frac{8}{7}$
			$f_{7/2}\rightarrow d_{5/2}$	$\sqrt{\frac{3}{7}}$	$\frac{20}{3}$	$\frac{50}{21}$	$\frac{15}{14}$
			$f\rightarrow d_{3/2}$	$\sqrt{\frac{3}{7}}$	7	2	$\frac{2}{7}$

evaluation of the atomic charge and magnetic multipole moments using the experimental data. We have compared the RIXS and RPES integrated cross sections to show that when the measurements are not sensitive to the emitted photon polarization or emitted electron spin direction, respectively, the sum rules in both theories differ only by some numerical factors regarding high-order multipole quantities, which can make (or not make) a significant difference depending on the particular approaches followed by the experimentalists in their applications. Moreover, for the application of the RIXS sum rules in the so-called perpendicular geometry using circularly polarized light we have provided detailed formulas and tables which constitute a complete framework for experimentalists to select the most useful scattering process and geometry for the case of interest.

ACKNOWLEDGMENTS

We are grateful to Lucio Braicovich and Alberto Tagliaferri for long-standing and enriching discussion on sum rules in RIXS and RPES.

APPENDIX A: DEFINITIONS OF SYMBOLS

We summarize here the most important definitions of the symbols occurring in Eq. (1). For other details, see Refs. 16, 23, and 30.

$$\mathbb{N}(l,L,L',\lambda,\lambda',\omega)=\frac{\lambda^2}{4}\frac{[L,L']}{[l]^{1/2}}|\mathcal{A}(\omega_{\mathbf{k}})^{L',\lambda'}_{L,\lambda}|^2, \quad \text{(A1)}$$

with $\lambda=|\mathbf{k}|^{-1}$.

$$\mathbb{E}^{zz'r}_{j_1}(c_1,l,L)=\sum_{ab}\tilde{\mathcal{C}}^{abrzz'}_{j_1}(c_1,l,L)\underline{w}^{abr}_0, \quad \text{(A2)}$$

$$\tilde{\mathcal{B}}^{z'}_{j_1,j_2}(c_1,c_2,L')=\frac{n_{L'z'}}{n_{j_1z'}[c_1][c_2]^{1/2}}\mathcal{B}^{z'}_{j_1,j_2}(c_1,c_2,L'), \quad \text{(A3)}$$

according to the definition of $\mathcal{B}^{z'}_{j_1,j_2}(c_1,c_2,L')$ in Eq. (23) of Ref. 23.

$$\Theta^{zz'r}(\hat{\mathbf{k}},\hat{\mathbf{k}}')=\sum_{\zeta}\left[C^{r0}_{z-\zeta,z'\zeta}\mathbb{C}^{z}_{-\zeta}(\hat{\mathbf{k}})\mathbb{C}^{z'}_{\zeta}(\hat{\mathbf{k}}')\right], \quad \text{(A4)}$$

with $\hat{\mathbf{k}}\equiv(\theta,\varphi)$ and $\hat{\mathbf{k}}'\equiv(\theta',\varphi')$. The $\mathbb{C}^{z}_{\zeta}(\theta,\varphi)$ are normalized spherical harmonics[40] while the $C^{r,0}_{z,-\zeta,z',\zeta}$ are Clebsch-Gordan coefficients.

The integer range of the most important indices is

$$a\in\{0,\ldots,2l\},$$

$$b\in\{0,1\},$$

$$r\in\{|a-b|,\ldots,(a+b)\}\ \text{and}\ \{|z-z'|,\ldots,(z+z')\},$$

$$\rho\in\{0\}\ \text{for}\ SO_2\ \text{symmetry},$$

$$z\in\{0,\ldots,2L\},$$

$$\zeta\in\{-z,\ldots,z\},$$

$$z'\in\{0,\ldots,2L'\},$$

$$\zeta'\in\{-z',\ldots,z'\},$$

and z' is even in the absence of spin- or light-polarization detection.

APPENDIX B: COEFFICIENTS FOR RIXS SUM RULES IN PERPENDICULAR GEOMETRY

Here we provide the required coefficients to compute Eqs. (3)–(6). The expressions for the coefficients $C_i\propto A_i\mathcal{B}^j$ for electric dipole and quadrupole transitions are listed in Table II. The factors A_i^{EL}, which differ for $E1$ and $E2$ excitations, are listed in Table III. They are a linear combination of $\mathbb{E}^{zz'r}$, which expressions are given in Table IV. The values of $\mathcal{B}^0$ and $\mathcal{B}^2$ are given in Table V, together with K_1 and K_2 required for the numerical factor $k=8\pi\lambda^2|\mathcal{A}(\omega_{\mathbf{k}})|^2K_1K_2/(256\pi^2)$.

*Electronic address: borgatti@tasc.infm.it
†Electronic address: giacomo.ghiringhelli@fisi.polimi.it

[1] G. Schütz, W. Wagner, W. Wilhelm, P. Kienle, R. Zeller, R. Frahm, and G. Materlik, Phys. Rev. Lett. **58**, 737 (1987).
[2] C.T. Chen, F. Sette, Y. Ma, and S. Modesti, Phys. Rev. B **42**, 7262 (1990).
[3] G. van der Laan, B.T. Thole, G.A. Sawatzky, J.B. Goedkoop, J.C. Fuggle, J.M. Esteva, R.C. Karnatak, J.P. Remeika, and H.A. Dabkowska, Phys. Rev. B **34**, 6529 (1986).
[4] J. J. Sakurai, *Advanced Quantum Mechanics* (Addison-Wesley, New York, 1967), p. 56.
[5] F. Gel'mukhanov and H. Ågren, Phys. Rev. A **54**, 3960 (1996).
[6] J. Luo, G.T. Trammell, and J.P. Hannon, Phys. Rev. Lett. **71**, 287 (1993).
[7] M. Magnuson, N. Wassdahl, A. Nilsson, A. Frölisch, J. Nordgren, and N. Mårtensson, Phys. Rev. B **58**, 3677 (1998)
[8] M. Finazzi, N.B. Brookes, and F.M.F. de Groot, Phys. Rev. B **59**, 9933 (1999).
[9] S.M. Butorin, J.H. Guo, M. Magnuson, P. Kuiper, and J. Nordgren, Phys. Rev. B **54**, 4405 (1996).
[10] L. Braicovich, C. Dallera, G. Ghiringhelli, N.B. Brookes, J.B. Goedkoop, and M.A. van Veenendaal, Phys. Rev. B **55**, R15989 (1997).
[11] M. Matsubara, T. Uozumi, A. Kotani, Y. Harada, and S. Shin, J. Phys. Soc. Jpn. **69**, 1558 (2000).
[12] F. Borgatti, P. Ferriani, G. Ghiringhelli, A. Tagliaferri, B. De Michelis, C.M. Bertoni, N.B. Brookes, and L. Braicovich, Phys. Rev. B **65**, 094406 (2002).
[13] B.T. Thole, P. Carra, F. Sette, and G. van der Laan, Phys. Rev. Lett. **68**, 1943 (1992).
[14] P. Carra, B.T. Thole, M. Altarelli, and X. Wang, Phys. Rev. Lett. **70**, 694 (1993).
[15] C.T. Chen, Y.U. Idzerda, H.J. Lin, N.V. Smith, E. Chaban, G. Meigs, G.H. Ho, E. Pellegrin, and F. Sette, Phys. Rev. Lett. **75**, 152 (1995)
[16] G. van der Laan and B.T. Thole, J. Phys.: Condens. Matter **7**, 9947 (1995).
[17] B.T. Thole, H.A. Dürr, and G. van der Laan, Phys. Rev. Lett. **74**, 2371 (1995).
[18] M. Finazzi, G. Ghiringhelli, O. Tjernberg, and N.B. Brookes, J. Phys.: Condens. Matter **12**, 2123 (2000).
[19] M. Taguchi and G. van der Laan, Phys. Rev. B **66**, 140401 (2002).
[20] H.A. Dürr, G. van der Laan, D. Spanke, F.U. Hillebrecht, and N.B. Brookes, Europhys. Lett. **40**, 171 (1997).
[21] M. Taguchi, G. van der Laan, E. Arenholz, S.S. Dhesi, and E. Dudzik, Phys. Rev. B **68**, 104408 (2003).
[22] P. Carra, M. Fabrizio, and B.T. Thole, Phys. Rev. Lett. **74**, 3700 (1995).
[23] M. van Veenendaal, P. Carra, and B.T. Thole, Phys. Rev. B **54**, 16010 (1996).
[24] L. Braicovich, G. van der Laan, G. Ghiringhelli, A. Tagliaferri, M.A. van Veenendaal, N.B. Brookes, M.M. Chervinskii, C. Dallera, B. De Michelis, and H.A. Dürr, Phys. Rev. Lett. **82**, 1566 (1999).
[25] K. Fukui, H. Ogasawara, A. Kotani, T. Iwazumi, H. Shoji, and T. Nakamura, J. Phys. Soc. Jpn. **70**, 1230 (2001).
[26] L. Braicovich, G. van der Laan, G. Ghiringhelli, A. Tagliaferri, and N.B. Brookes, Phys. Rev. B **66**, 174435 (2002).
[27] L. Braicovich, A. Tagliaferri, G. van der Laan, G. Ghiringhelli, and N.B. Brookes, Phys. Rev. Lett. **90**, 117401 (2003).
[28] G. van der Laan and B.T. Thole, Phys. Rev. B **52**, 15355 (1995).
[29] P. Carra and M. Fabrizio, in *Core Level Spectroscopies for Magnetic Phenomena: Theory and Experiment*, edited by P. S. Bagus, G. Pacchioni, and F. Parmigiani (Plenum Press, New York, 1995).
[30] P. Ferriani, Ph.D. thesis, Università di Modena e Reggio Emilia, 2002.
[31] P. H. Butler, *Point Group Symmetry: Applications, Methods and Tables* (Plenum, New York, 1981).
[32] P. Carra and B.T. Thole, Rev. Mod. Phys. **66**, 1509 (1994).
[33] For ease of comparison we give the conversion table for the parameters appearing in the two different theories. In this work we follow the notation from Ref. 23.

This work (RIXS): w, a, b, r, z, z', L, μ, $\mathbf{k}$, $\mathbf{k}'$, c_1, j_1, l, Θ
Ref. 16 (RPES): w, x, y, z, a, r, Q, q, $\mathbf{P}$, ε, c, j, l, U
There is a one-to-one correspondence between parameters in the same column.

[34] G. van der Laan, Phys. Rev. B **57**, 112 (1998).

[35] We have adopted here the hole operators $\underline{w}^{abr}$ defined in Ref. 23 rather than the electron operators w^{abr} chosen in Ref. 34. The relation between the two is $\underline{w}^{abr}=(-1)^r w^{abr}$ for all r except $\underline{w}^{000}=(4l+2)-w^{000}$.

[36] It should be noted that the results are independent of the principal quantum number (n) of the levels involved, apart from a scaling factor common to J_{sum} and J_{dif}. Moreover, it is assumed that j is a ''good'' quantum number for the core levels with a hole in the intermediate state.

[37] G. Ghiringhelli, Ph.D. thesis, Université Joseph Fourier-Grenoble I (2001), www.dissertation.de

[38] K. Fukui, H. Ogasawara, A. Kotani, T. Iwazumi, H. Shoji, and T. Nakamura, J. Phys. Soc. Jpn. **70**, 3457 (2001).

[39] A. Tagliaferri, G. Ghiringhelli, G. van der Laan, N. B. Brookes, and L. Braicovich (unpublished).

[40] D. A. Varshalovich, A. N. Moskalev, and V. K. Khersonskii, *Quantum Theory of Angular Momentum* (World Scientific, Singapore, 1988).